Petrosamine Revisited. Experimental and Computational Investigation of Solvatochromism, Tautomerism and Free Energy Landscapes of a Pyridoacridinium Quaternary Salt.

Christopher J. Gartshore , Yongxuan Su * , Tadeusz F. F. Molinski *

Posted Date: 14 July 2023

doi: 10.20944/preprints202307.0956.v1

Keywords: Alkaloid; pyridoacridine; acetylcholine esterase, merocyanine, marine natural product; NMR; UV-vis spectroscopy.

Article

Petrosamine Revisited—Experimental and Computational Investigation of Solvatochromism, Tautomerism and Free Energy Landscapes of a Pyridoacridinium Quaternary Salt

Christopher Gartshore [1], Yongin Su [1] and Tadeusz F. Molinski [1,2,*]

[1] Department of Chemistry and Biochemistry, University of California, San Diego, 9500 Gilman Drive, La Jolla, CA 92093, USA MC3568; gartcj@gmail.com

[2] Skaggs School of Pharmacy and Pharmaceutical Sciences, University of California, San Diego, 9500 Gilman Drive MC3568, University of California, San Diego, 9500 Gilman Drive, La Jolla, CA 92093, USA.

* Correspondence: tmolinski@ucsd.edu

Abstract: Petrosamine (**1**) – a colored pyridoacridine alkaloid from the Belizean sponge, *Petrosia* sp. that is also a potent inhibitor of acetylcholine esterase (AChE) – was investigated by spectroscopic and computational methods. Analysis of the petrosamine free energy landscapes, pK_a and tautomerism revealed an accurate electronic depiction of the molecular structure of **1** as the di-keto form, with net charge of q = +1, rather than a dication (q = +2) under ambient conditions of isolation-purification. The pronounced solvatochromism (UV-vis) reported for **1**, and related analogs, was investigated in detail and is best explained by charge delocalization and stabilization of the ground state (HOMO) of **1** rather than an equilibrium of competing tautomers. Refinement of the molecular structure of **1** by QM methods complements published computational docking studies to define the contact points in the enzyme active site that may improve design of new AChE inhibitors based on the pyridoacridine alkaloid molecular skeleton.

Keywords: alkaloid; pyridoacridine; acetylcholine esterase; merocyanine; marine natural product; NMR; UV-vis spectroscopy

1. Introduction

In 1988, Molinski and Faulkner reported the structure of petrosamine (**1**), a highly condensed pentacyclic alkaloid of intense color that was isolated from the sponge, *Petrosia* sp., collected at Carrie Bow Cay, Belize [1]. Although no bioactivity of **1**was reported at the time, a pronounced solvatochromism – the property of color changes (l_{max}) in solvents of different polarities – was observed. At the time, **1** represented the most complex structure in a growing class of pyridoacridine alkaloids from marine invertebrates [2]. Structurally, **1** can be considered an methylated and oxidized analog of the pentacyclic amphimedine – the first member of this class of alkaloid, described by Schmitz and co-workers in 1983 [3]. Unlike the structures of most pyridoacridines where the 3 nitrogen atoms are sp^2 hybridized, **1** contains a quaternary ammonium salt with an sp^3 quaternized N. Pyridoacridines manifest a range of biological activities including cytotoxicity, antineoplastic properties, antibacterial activity, and enzyme inhibition; a subject that has been extensively reviewed [4].

Since its initial report, alkaloid **1** has been reisolated from a Thai species of sponge, *Petrosia* n sp.[5], and two new analogues have been described; petrosamine B (**2**) [6] a regioisomer of **1** from the Australian sponge *Oceanapia* sp. with modest inhibitory activity against aspartate semialdehyde dehydrogenase, and debromopetrosamine (**3**) from *Xestospongia* cf *carbonaria* collected in Palau [7]. Numerous marine natural products have been reported with neuroprotective properties in experimental models for neurodegenerative diseases including acetylcholine esterase (AChE) inhibition [8]. Suwanborirux and coworkers showed that **1** is a potent inhibitor of AChE from the Pacific electric ray, *Torpedo californica* (IC_{50} = 91 nM) [**Error! Bookmark not defined.**]; approximately

Preprints (www.preprints.org) | NOT PEER-REVIEWED | Posted: 14 July 2023 doi:10.20944/preprints202307.0956.v1

6 times more potent than galanthamine (**4**), an alkaloid used in the past for treatment of patients with Alzheizmer's disease (AD) to compensate neurotransmitter deficiency.

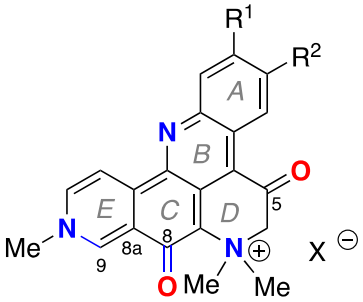

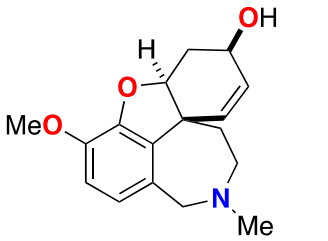

4 Galanthamine

R^1 = Br, R^2 = H, X = Cl^- **1** Petrosamine
R^1 = H, R^2 = Br, X = CF_3COO^- **2** Petrosamine B
R^1 = R^2 = H, X = CF_3COO^- **3** Debromopetrosamine

Preliminary docking studies of **1** with AChE revealed subtle electronic interactions with the putative receptor contacts [**Error! Bookmark not defined.**]. Given the global rise of AD within aging populations and the therapeutic importance of AChE inhibitors for treatment, a detailed understanding of the electronic structure and molecular parameters for enzyme-inhibitor molecular contacts of **1** may advance design principles for new AD therapeutics. In this report, we present refined measurements of UV-vis, *p*K$_a$ properties and quantum mechanical calculations of **1** that relate the observed solvatochromism through mapping of dipolar resonance forms to a simple model based on merocyanine dyes, and stabilization of the ground state of the HOMO.

Petrosamine (**1**) exhibits several unusual physical and spectroscopic properties. The melting point of **1** is in excess of 300 °C suggesting high stabilization within the lattice energy of the crystalline form. Unlike most other pentacyclic pyridoacridines, the color of **1** is strikingly variable depending upon the physical state. Crystals of **1** are deep blue-purple but dilute solutions of **1** show highly complex UV-vis spectra due to the presence of long wavelength absorption bands that manifest pronounced solvatochromism (changes in l_{max} of **1** when measured in different solvents). For example, solutions of **1** in MeOH appear deep-blue (longest l_{max} = 595 nm), but aqueous solutions of **1** appear purple l_{max} = 574 nm) [**Error! Bookmark not defined.**]. In dilute THF solutions (sparingly soluble) or DMSO, **1** appears green l_{max} = 611 nm) [**Error! Bookmark not defined.**]. In short, the range Δl_{max} of **1** is 36 nm in a range of solvents from H_2O to DMSO. Petrosamine also displays pH indicator properties: addition of excess alkali to purple aqueous or blue MeOH solutions of **1**, changes the color to green, suggestive of a hypsochromic shift ($\Delta l_{max} < 0$) mediated by the Brønsted acidity of the a-CH_2 next to the keto group and deprotonation to the corresponding enolate.

In the report by Quinn and coworkers describing isolation of **2** by "fractionation on C18" and elution with a stepped gradient of acidic (CF_3COOH) aqueous-MeOH [**Error! Bookmark not defined.**], also reported solvatochromism in **2** very similar to that of **1**. Assignment of the structure of **2** was achieved through extensive analysis of ^1H, ^{13}C NMR and 2D NMR data (D_2O-TFA-1% DMSO-d_6). Compound **2** was depicted as a dication different from **1** in the resonance form of an O-protonated vinylogous amide embodying a fully aromatic quinolinium ring E [**Error! Bookmark not defined.**]. Additional structural anomalies emerged. The assignment of C-8 in **2** is supported by an HMBC correlation from H-9 to C-8 ($^3J_{CH}$) based on the low ^{13}C NMR chemical shift (*d* 155.8 ppm), but no inter-ring HMBC correlations were reported for C-5 [**Error! Bookmark not defined.**]. In contrast, the X-ray crystal structure of **1** [**Error! Bookmark not defined.**] clearly reveals two keto groups in the solid state (*d* (C-8–O) = 1.256 Å; *d* (C-5–O) = 1.203 Å), *d* (C-5–C-6) =1.495(21). The C-O and C-C bond lengths are only compatible with a di-keto structure [9]. As the structures of **1** and **2** are very similar; consequently, the solution properties (*p*Ka, UV-vis) should be also closely matched. Faulkner and Molinski reported the ^{13}C NMR spectra (DMSO-d_6) of **1**, but not the assignments of the signals [**Error!**

 doi:10.20944/preprints202307.0956.v1

Bookmark not defined.]. Suwainborix and coworkers, reporting the ^{13}C NMR spectrum of **1** in the latter solvent, assigned the signal at *d* 161.3, s, the higher-field of the two most deshielded signals (*d* 187.2, s; 161.3, s) to C-8 [**Error! Bookmark not defined.**])

Comparisons of the NMR assignments of **1** and **2** are complicated further by measurements in different solvents, and possible changes in tautomer or enolization states that accompany changes in pH and NMR solvent polarity, and H-bond donor-acceptor properties of the alkaloids. Clearly, the latter factors affect the UV-vis properties of **1** and **2**. Surprisingly, neither the Quinn [**Error! Bookmark not defined.**] or Suwainborix [**Error! Bookmark not defined.**] groups claim to have observed the rapid enolization of **1** in D_2O reported by Faulkner and Molinski that resulted in complete deuteriation of C-9 and 'loss' of the C-9 signal [**Error! Bookmark not defined.**,10].

In order to reconcile these apparent paradoxes, it is required that a re-examination of **1** be given separate considerations of resonance in the native structure, and possible tautomerism of **1** at the a-CH_2 next to the C-5 C=O group. We undertook the task and completed additional solution spectroscopic measurements of **1** [NMR and electronic spectroscopy, UV-vis] and MS time-course studies and augmented by quantum mechanics calculations. The results, presented here, clarify several phenomena of **1** including solvent-dependence of HOMO-LUMO energies, and kinetic and thermodynamic considerations of pK_a, and tautomerism.

2. Results and Discussion

The solvatochromism of **1** and **2** is similar to lower-order merocyanine dyes, the canonical substructures of which can be discerned within the molecular framework of both natural products (**Figure 1**). For example, the same conjugated sub-structure in Brooker's merocyanines [11,12] [generalized by Brooker as the vinylogous amide; neutral ***ia*** and ***ib*** dipolar (zwitterionic) resonance forms] is embedded in the molecular frameworks of **1** and **2**. Brooker merocyanines, for example **5b** and **6b** (**Figure 1**) exhibit strongly positive solvatochromism (hypsochromism, or a blue shift in l_{max} in polar solvents). It is not unreasonable to invoke the same spectroscopic and electronic properties of **5** – zwitterionic form with extended conjugation, and stabilization of the ground state by solvation in polar solvents – as necessary and sufficient conditions to explain the solvatochromism of **1**–**3**.

While a complete description of electronic properties of petrosamine (**1**) may be achieved in rigorous quantum mechanical calculations (see below), it is helpful for visualization purposes to consider Lewis bond formalism and resonance structures [13]. For clarity, only two pairs of resonance forms are depicted for **1** to illustrate the zwitterionic contributions of merocyanine substructures: the non-charged resonance forms **1a**,**c**, and 'zwitterionic' resonance form **1b**,**d**. Forms **1a,b** depict the shorter bond path (n = 3, c.f. ***ia***, ***ib***, **Figure 4**) and dipolar resonance forms **1c,d** show a longer bond path in an 'aza-vinylogous amide' (n = 4). The shortest bond path, n = 1 (not shown) would involve only the atoms C-8–C8a–C9–N-10), while the longest path, n = 4, evoking 'particle-in-a-box' formalism [14], best explains the long-wavelength UV-vis bands of **1** giving rise to its colors.

Preprints (www.preprints.org) | NOT PEER-REVIEWED | Posted: 14 July 2023 doi:10.20944/preprints202307.0956.v1

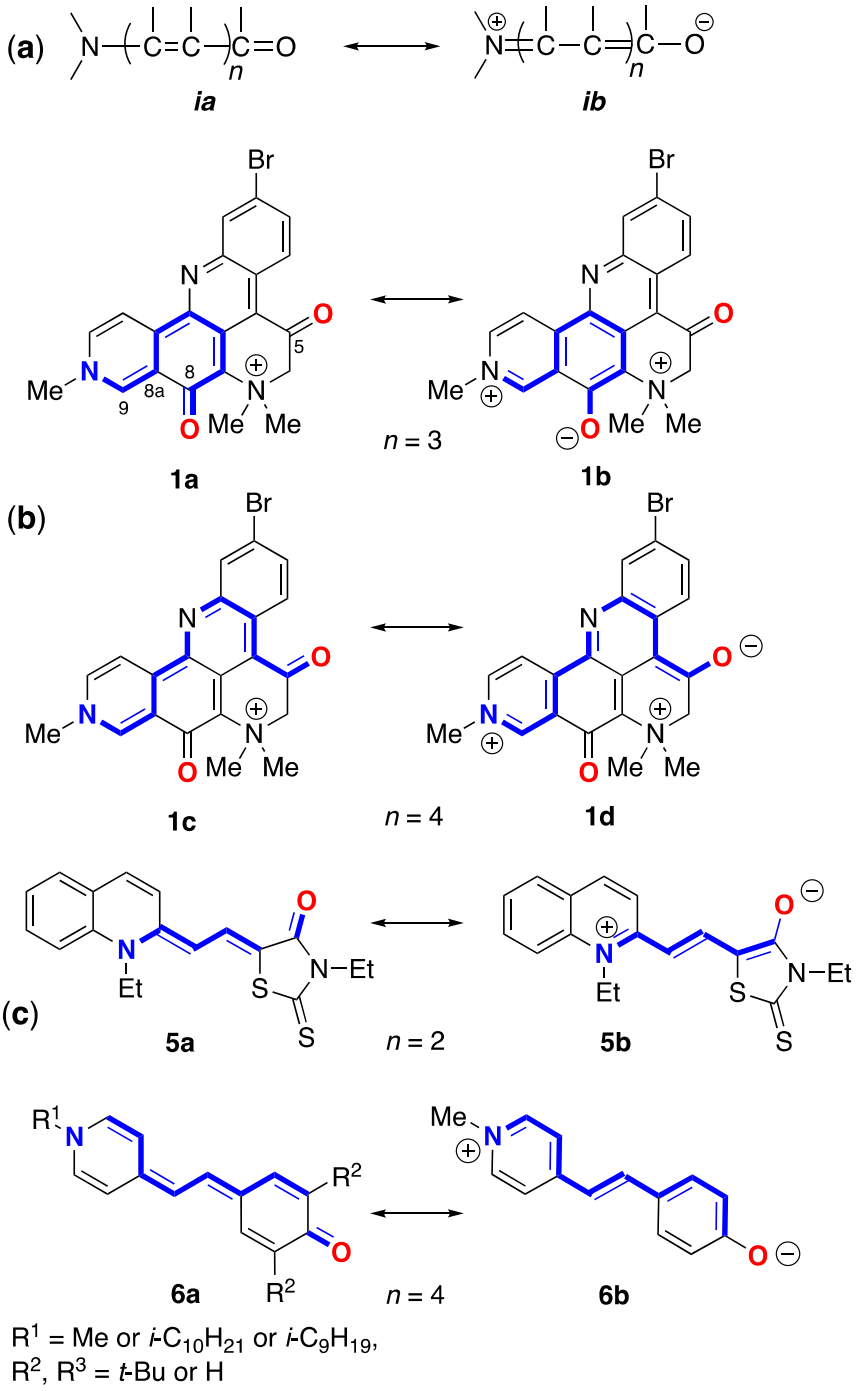

Figure 1. Canonical resonance forms – neutral (**a**) and dipolar (**b**) – for merocyanines defined by bond path, *n* (see [**Error! Bookmark not defined.**]). (**b**) Petrosamine 'neutral' and dipolar resonance forms: **1a** (*n* = 3), **1b** (*n*= 2), **1c** (*n* = 4) and **1d** (*n* = 4). (**c**) Brooker merocyanine resonance forms; neutral (**4a**, **5a**, **6a**) and dipolar (**4b**, **5b**, **6b**) forms [**Error! Bookmark not defined.**].

Solvatochromism of Brooker merocyanines has been rationalized [**Error! Bookmark not defined.**b], using semi-quantitative valence resonance and frontier orbital theories, as arising from more extensive stabilization of the dipolar form **4a** of the ground state relative to the excited state in polar solvents. Accordingly, this differential stabilization gives rise to an increase in the electronic transition energy, ΔE, due to a larger gap between the HOMO and LUMO of the longest wavelength transitions. The HOMO-LUMO gap is predicted to increase (blue shifted absorption) in those structures with higher contributions from the zwitterionic resonance form **4b**, leading to more pronounced solvatochromism. More recent semi-empirical calculations (COSMO, PM3) of a different set of substituted Brooker merocyanines (**5**) by Morley and coworkers [15] supported stabilization of

Preprints (www.preprints.org) | NOT PEER-REVIEWED | Posted: 14 July 2023 doi:10.20944/preprints202307.0956.v1

the ground state as mostly responsible for solvatochromism and predicted a larger role for hydrogen bonding in the zwitterionic form **5b** over the neutral form **5a**.

The structure of petrosamine (**1**) appears to fulfill the criteria for merocyanine-type solvatochromism. Measurements of the UV-vis spectrum of solutions of **1** prepared in DMSO–H_2O solvents of variable composition (**Figure 2**) exhibit changes in the l_{max}. Most prominently, the longest wavelength absorption band with the largest hypsochromic shift between 100% DMSO and100% H_2O (Δl_{max} –78 nm) is assigned to the forbidden n–π* transition that lends color to **1**, analogous to that of merocyanines.

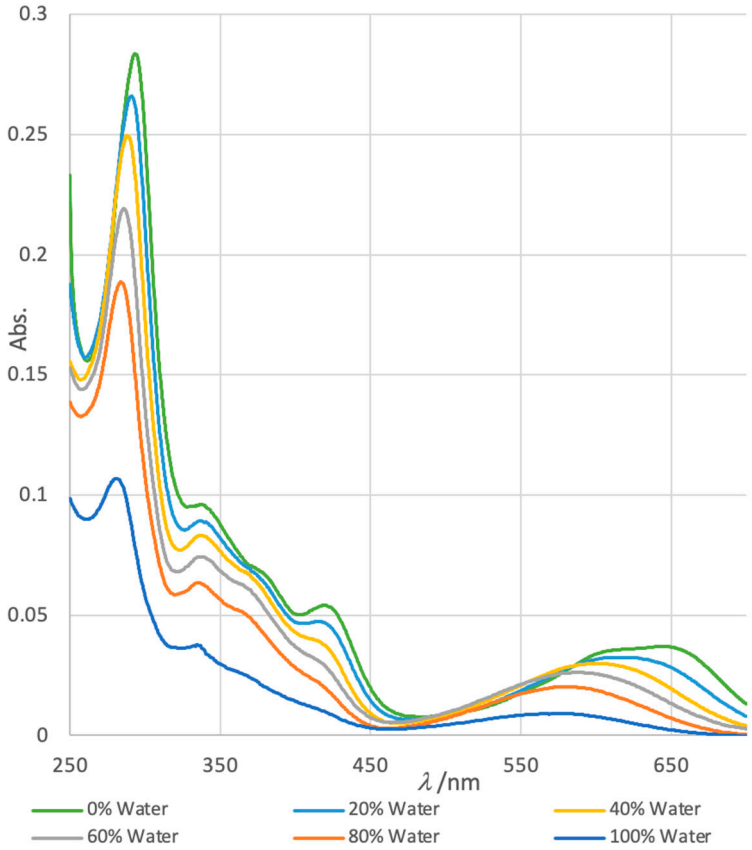

Figure 2. Solvatochromism in normalized electronic UV-vis spectra of petrosamine (**1**) in H_2O-DMSO solvents of variable composition (H_2O v/v = 0%, 20%, 40%, 60%, 80% and 100%).

A clear trend emerges: band-1 (l_{max1}, defined here for convenience, as the dominant π-π* transition) shows a dramatic decrease in e with increasing H_2O content of the solvent, and a weak bathochromic shift between 100% H_2O to 100% DMSO (Δl_{max1} 15 nm, **Table 1**). In contrast, the corresponding changes in band-2 include a strong blue-shift (hypsochromism, l_{max2} –78 nm). The band l_{max2} is affected most by solvents with increasing H_2O content which parallels the reported behavior of Brooker merocyanines.

Table 1. UV-vis properties of l_{max1}[1] and l_{max2}[1] in petrosamine (**1**) in DMSO-H_2O.[1.]

% H_2O *v/v*)	l_{max1} (nm)	e_1[1]	l_{max2} (nm)	e_2[1]
0	281	68,500	648	24,000
20	282	122,252	622	20,600
40	287	141,700	604	19,400
60	288	161,000	589	16,500
80	290	172,000	581	12,900
100	296	184,000	570	4,700

[1] See text for definitions. [1.]e values normalized from the literature value of l_{max2} (e 4,700) [**Error! Bookmark not defined.**].

Preprints (www.preprints.org) | NOT PEER-REVIEWED | Posted: 14 July 2023 doi:10.20944/preprints202307.0956.v1

For comparison, we prepared the known merocyanine **6b** from 4-methylpyridine by the following sequence adapted from Minch and Sadiq Shah:[16] methylation (MeI, *i*PrOH, reflux), condensation of the resultant pyridinium methiodide with *p*-hydroxybenzaldehyde (piperidine, EtOH, reflux), and neutralization of the product **7** (nBu$_4$N$^+$ HO$^-$) to zwitterionic phenolate **6b**. Measurements of the UV-vis spectra of **6b** (nBu$_4$N$^+$ salt) in mixed solvents (acetone-H$_2$O, see Supporting Information) showed a hypsochromic trend similar to that of **1** in DMSO-H$_2$O. The long-wavelength **(**band-2) varied from l_{max}(acetone) 591 nm to l_{max} (H$_2$O) 444 nm (Δ l_{max} –69 nm) while e changed only slightly across the range of solvent mixtures [17].

2.1. *QM Calculations*

The energies of electronic states of **1** were calculated using QM methods (DFT). Starting with the X-ray coordinates of **1**, the geometry of the structure was first minimized using MMFF, then further refined by DFT (B3LYP 6-31G*, polarization continuum model = H$_2$O). The 3D model of **1**, overlaid with frontier MOs, is shown in **Figure 3**. As expected, the ΔE for the HOMO-LUMO gap is relatively small (ΔE = xx eV). The orbital coefficients and calculated dipole moment of the excited state (μ = 18.5 D) are consistent with dominant contributions from the resonance form **1b** rather than **1a**, and the strong donor properties of N-10. At first this may seem anomalous, given the relatively low-field ^{13}C NMR signal measured for C-5 in **1** (d 187.4 [**Error! Bookmark not defined.**] or 187.2 in **2** [**Error! Bookmark not defined.**]) however, the additional deshielding effect is likely attributed to the inductive effect of the quaternized N-7.

The electrostatic potential map of the minimized structure of **1** (**Figure 4**) clearly shows two loci of positive charge: one centered on the quaternized N-10, as expected, in ring D, and a second associated with the N atom in ring E. The latter supports charge separated forms **1b**,**d** (Figure 1) in which N-10 participates as a donor group. Consequently, the formal bonding electron pair of N-10 is highly delocalized and can confer only weak basicity to **1**. Together with the UV-vis properties of **1**, the overall electron delocalization consolidates an electronic structure in which a zwitterionic partial structure strongly lends to charge-separation mostly in the ground state.

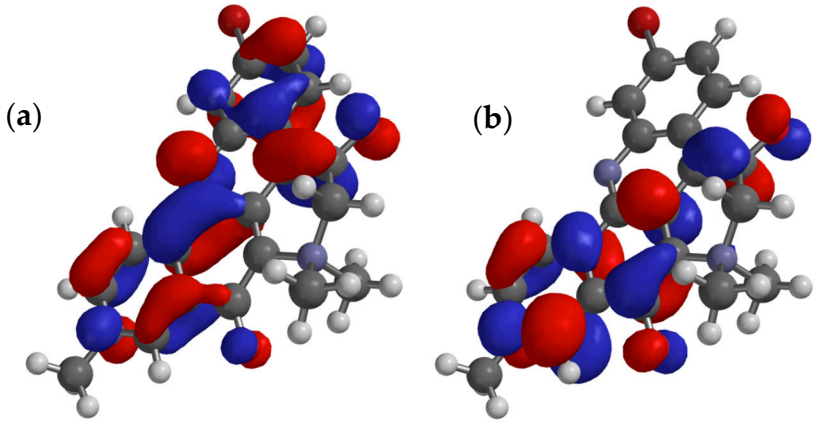

Figure 3. Calculated minimized structure and overlaid frontier π-orbitals of petrosamine (**1**) (DFT B3LYP 6-31G*, polarization continuum model = H$_2$O) (a) HOMO and (b) LUMO.

From an empirical viewpoint, the latter makes sense as the charge-separated forms **1b,d** preserve the aromaticity of rings A and E. A result of this delocalization is reduced basicity of N in ring E and, consequently, an expected lower pK$_a$ for the conjugate Brønsted acid. Formally, addition of H$^+$ **1** to give a dication should sooner favor the C-8 or C-5 oxygen as an acceptor, rather than N-10 or N-13. In fact, we find no evidence (NMR) for protonation of **1** at pH ~ 2, which attests to the overall poor basicity of **1**; an unsurprising finding given the permanent formal charge of +1 in this quaternary ammonium salt in all but the most basic or the most acidic media.

Preprints (www.preprints.org) | NOT PEER-REVIEWED | Posted: 14 July 2023 doi:10.20944/preprints202307.0956.v1

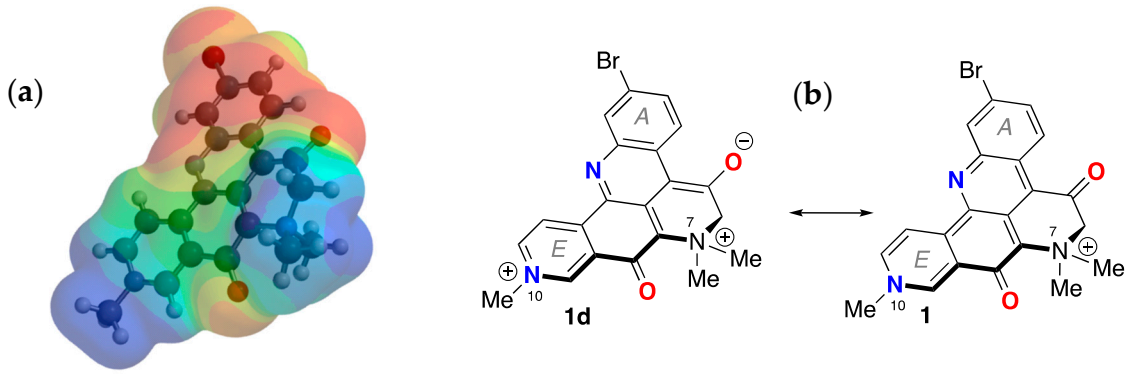

Figure 4. Minimized energy structure of petrosamine (**1**, DFT, EDF2 6-31G, dipole moment μ = 18.5 D). (**a**) electrostatic potential surface and (**b**) the corresponding molecular framework of **1** (dipolar **1d** and 'charge-minimal' **1** resonance forms).

2.2. *pK_a of Petrosamine (1). Does the structure of 1 exhibit substantial enol content?*

In order to estimate the pK_a of petrosamine, the UV-vis spectra of **1** were measured in buffered D_2O at different pH. The titration curve of **1** (S1) shows little change in the UV-vis spectra in the range of pH 2 – 10. From the Henderson-Hasselbach relationship (Equation (1))[18] for Brønsted acid HA, the condition pH = pK_a is met when concentrations of conjugate species are equal ([HA] = [A^-]). We surmise the pK_a of **1** lies outside this pH range (pK_a >10). Indeed, a bathochromic shift in the UV-vis spectrum of **1** is only observed when a methanolic solution is treated with high concentrations of NaOH (2M, pH >13). Conversely, only when a sample of **1** is dissolved in a very strong Brønsted acid (neat CF_3COOH) are conditions met for a reasonable expectation of, diprotonated petrosamine ([**1**•2H]$^{2+}$). In the event, when **1** was dissolved in neat TFA, the blue-purple color changed to bright yellow. The latter observation contrasts with the supposition drawn by Quinn and coworkers of doubly-protonated petrosamine B ([**2**•2H]$^{2+}$) from their observation that **2** remains *"bright blue…when dissolved in methanol"*, under the relatively benign conditions used in C_{18}-reversed phase isolation of the alkaloid (5% TFA-MeOH) [**Error! Bookmark not defined.**]. In other words, N-10 in the monocationic molecules **1**-**3** is 'pyridinium-like' and non-basic (resembling **1d**), and the C-8 C=O is insufficiently Brønsted-basic to be substantially protonated under ordinary isolation conditions.

$$\mathrm{pH} = \mathrm{p}K_a + \log_{10}[A^-]/[HA] \qquad (1)$$

It is evident from the ^1H and ^{13}C NMR (DMSO-d_6) that C-5 in petrosamine (**1**) is in the C8 keto form, a conclusion also reached by both the Suwanborirux and coworkers [**Error! Bookmark not defined.**], and independently by Quinn and coworkers for petrosamine B (**2**) [**Error! Bookmark not defined.**]. The single crystal X-ray crystallography of **1** is concordant with the C8 keto form. In fact, solid state **1** is best represented by the di-keto tautomer, e.g. interatomic distances C8-O2, 1.256(17) Å; C5-O1, 1.203(15), and C5-C6, 1.495(21) [**Error! Bookmark not defined.**].

2.3. *Kinetic Measurements of Hydrogen-Deuterium Exchange of 1*

None of the resonance forms of **1a-d (Figure 1)**– or more precisely, pathways of electron delocalization – explain the complete exchange of the H-6 protons by deuterium when **1** was dissolved in deuteric solvents (D_2O, CD_3OD) [**Error! Bookmark not defined.**]. The latter can only be rationalized by consideration of the possibility of enolization (**Figure 6**), either through the positively charged **8a** in neutral to weakly acidic pH or the charge-neutral (zwitterionic) enolate **8b** under highly basic pH. The kinetic parameters for successive H replacement by D in **1**, defined by rate constants k_1 and k_2, are intrinsic properties as opposed to thermodynamic properties that relate to the equilibrium constants K_{eq1} and K_{eq2}; the latter are largely dependent upon the strength and concentration of added base, B^- (**Figure 6**).

Preprints (www.preprints.org) | NOT PEER-REVIEWED | Posted: 14 July 2023 doi:10.20944/preprints202307.0956.v1

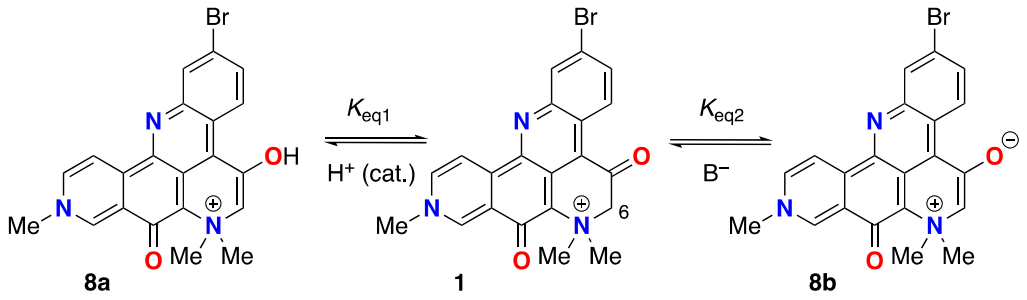

Figure 6. Keto-enol tautomerism of **1**. Enol **8a** (acid -catalyzed), and enolate **8b** (base-promoted).

In hydroxylic solvents, **1** also resides largely in the di-keto form, however, we found that in both D_2O and CD_3OD, the C-6 methylene protons undergo rapid exchange to give the C-6 CD_2-isotopomer (**1**-d_2) [**Error! Bookmark not defined.**]; a rate so fast that we were unable to detect the C-6 CH_2 or the intermediate forms within the time frame between sample preparation and measurement of the ^1H NMR spectra. This observation was supported by ^1H NMR, HSQC and HMBC measurements of **1** in protic solvent (CD_3OH) where the C-6-CH_2 group is still observable (HSQC correlation: H-6 to C-6, d_H 4.64, s; d_C 70.4 ppm). The simplest explanation for both phenomena is catalytic H-D exchange a-to the C-5 C=O group favored by an intermediate; the extensively-conjugated enol tautomer **8a** (**Figure 6**).

In order to estimate the rate of H-D exchange in **1** and place an upper bound on it, we measured the time-dependent appearance of the CD_2-isotopmer by ESI mass spectrometry after rapid dissolution of **1** in CD_3OD (**Figure 7**). Under controlled conditions (23 °C, rapid sampling and ESIMS in situ measurement- see Experimental), **1** ($C_{21}H_{17}{}^{89}BrN_3O_2$, m/z 422.0499 [M^+]) rapidly disappeared, followed by replacement by ephemeral isotopologue **1**-d_1 (m/z 423.0561) and finally, convergence upon **1**-d_2 (m/z 424.0624). Remarkably, complete exchange (>90%) is observed within 90 s of dissolution of **1.** From triplicate measurements, and rapid sampling (first measurement at t = 15 sec), we were able to fit the kinetic deuterium exchange data to a first order rate law and estimated the apparent first and second H-D exchange rate constants to be (**Table 2**), k_1= 0.1394(7) s^{-1} and k_2 = 0.0765(47) s^{-1} (best R^2; see Supporting Information). As expected, k_2 is about half of k_1, consistent with the expected rate laws, and negates involvement of a substantial kinetic isotope effect for the exchange reaction.

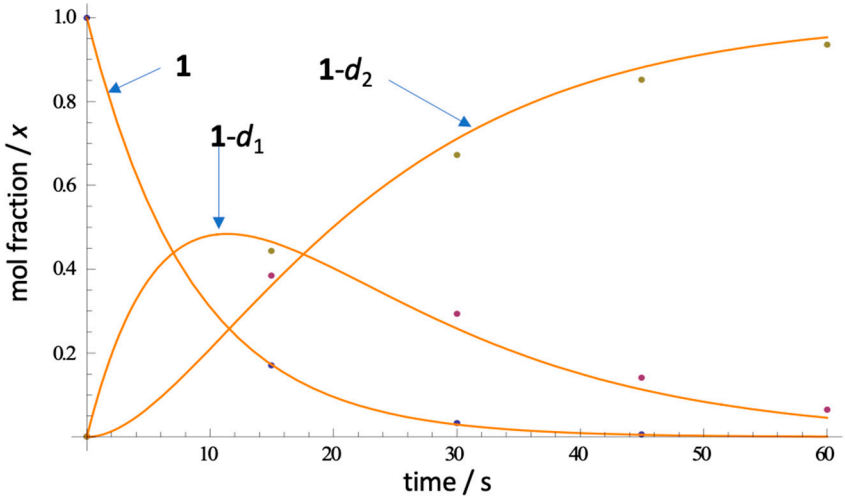

Figure 7. Representative ESIMS measurements of the rate of H-D exchange of petrosamine (**1** in CD_3OD, 23 °C) and fitted curves (non-linear regression). See Supp. Info. for rate law and k determinations.

Preprints (www.preprints.org) | NOT PEER-REVIEWED | Posted: 14 July 2023 doi:10.20944/preprints202307.0956.v1

The exchange of **1** to **1**-d_2, in the absence of added acid, appears to be much faster than H-D exchange rates of other phenones, e.g. propiophenone (pK_a 24.4, DMSO [19] a-tetralone (pK_a 24.7 [20,21]. The rates of acid-promoted keto-enol equilibration of acetophenone (pK_a 18.4±0.03) have been measured. For example, the rate of ketonization of acetophenone enol (1-phenylethen-1-ol) is linearly dependent upon [H_3O^+] with a catalytic efficiency determined to be k_{H+} = (1.25±0.02) x 10^3 $M^{-1}s^{-1}$ [22]. We conclude that tautomerism of **1** too must be very fast even in the absence of added acid. Either the enol **8a** or enolate **8b,** although undetectable as a discrete species in the time frame of ^{1}H NMR, present a pathway to the acid-base equilibria of **1** and **1**-d_2, but enolization of the keto form is likely dominant.

Table 2. Rate constants k_1 and k_2 for H-D exchange in **1** in CD_3OD (23° C, see **Figure 5**).[1]

Reaction	k_1 (s^{-1})	k_2 (s^{-1})
1 –> **1**-d_1	0.1394(7)	–
1-d_1 –> **1**-d_2	–	0.0765(47)

[1] See Supporting Information for plotted raw ESIMS data and detailed kinetic analysis.

Some amount of discussion has been given on the keto-enol state of **1.** The NMR data for **1** reported by Suwainborirux and coworkers support the C5 keto form in DMSO-d_6 [**Error! Bookmark not defined.**] and – in agreement with Molinski and Faulkner, the enol form in D_2O or CD_3OD [**Error! Bookmark not defined.**] – but Quinn and coworkers find, "*no evidence for this keto-enol isomerism*" in **2**. [1] Likely, the K_{eq} of keto-enol tautomerism lies on some continuum, dependent upon solvent dialectric and H-bond donor ability.

The observed ^{1}H and ^{13}C NMR spectra of petrosamine (**1**), and the C6 exchange to CD_2 in CD_3OD/NaOD, support the enol form in hydroxylic solvents. It's likely fast exchange hybrid structure of **1** and **8a,b** with an equilibrium constant K_{eq1} largely in favor of **1** in DMSO-*d*6, moving to the dominant **8a** in hydroxylic solvents. The enolate **8b** may be favored as the catalytically important intermediate, for reasons of charge neutralization, but insufficient data can support this hypothesis with more certainty. In either case – enol or enolate intermediate – we surmise the electron-withdrawing quaternized N^+Me_2 group in **1** and the related petrosamines, **2, 3**, plays an significant role in accelerating the rates of H-D exchange and lowering the pK_a of the C-6 CH_2 group.

To the best of our knowledge, rapid H-D exchange of a substituted b-quaternary ammonium ketone within a natural product has been observed only in one other instance, coulteroberbinone (**7**, **Figure 8** [23]), an *N*-quaternary ammonium isoquinoline alkaloid from the leaves of *Romneya trichocalyx*. The authors note the C-14 C-H in **7,** assigned to the α-proton between the carbonyl and quaternized nitrogen (d_H 5.64, s), underwent rapid proton-deuterium exchange in D_2O or CD_3OD to C-D (**7**-d_1) under ambient conditions (supported by ^{1}H NMR and ESIMS data).

1. We find it unlikely that the position of the Br in ring *A*– the only difference between **1** and **2** – would exert such a profound difference in behaviour. Quinn's argument is confounded by two uncertainties: the composition of their NMR solvent (TFA, D_2O, DMSO-d_6) is not specified quantitatively, and facile interpretation of the ^{13}C NMR signals for the C8 signal: "*in contrast C-8 resonated at 155.8 ppm, supporting it as a phenolic resonance. It was therefore more likely that petrosamine also exists in the C-8 enol form and C-8* [Molinski and Faulkner [**Error! Bookmark not defined.**]] *was the carbon at 161 ppm*", contrasts with those of Suwainboriruix (δ 174.7 ppm, DMSO-d_6) and their observation of, "*the broad methylene carbon at* δ_C *69.2" (DMSO-*d_6*, "100 μmol NaOD"*[**Error! Bookmark not defined.**]. Aside from these points, none of the three different ^{13}C NMR values for C8 in **1** and **2** are incompatible with the structures, both of which are not strictly aryl ketones but vinylogous amides. This is especially so given with solvent-dependence of electron-delocalization.

Preprints (www.preprints.org) | NOT PEER-REVIEWED | Posted: 14 July 2023 doi:10.20944/preprints202307.0956.v1

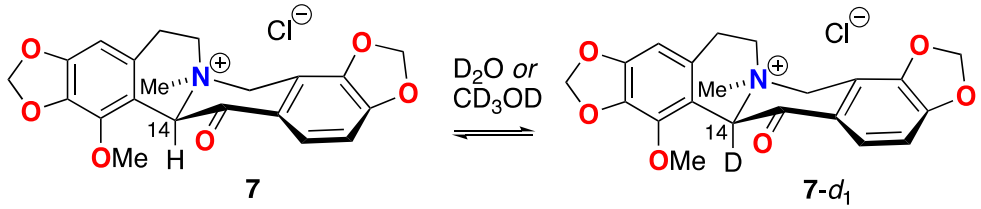

Figure 8. Rapid H-D exchange of coulterberbinone (**7**) in deuteric solvent under ambient conditions.

Two major factors most likely explain the relatively low pK_a of **1** and **7**: the electron withdrawing (inductive) effect of the -N^+Me_2 quaternary ammonium group (N-7) and stabilization of enol **5** (or enolate **6**) through extensive conjugation of the heteroaromatic core, not unlike the stabilization of the enolates of alkyl phenones, e.g. acetophenone, determined by UV-vis (*p*K_a = 18.4). Indirect determinations of the pK_a of the enol of acetophenone has also be obtained from kinetics of reactions of acetophenone: e.g. a-chlorination [24], and aminolysis of the corresponding enol acetate [25]. In contrast, **1** appears to undergo rapid enolization in the *absence* of added Brønsted acid, suggesting the possibility that this tautomerization that may even be autocatalytic.

Is the enol **8a** of petrosamine (**1**) present in substantial concentrations? From the ^{1}H NMR spectrum of **1,** (DMSO-d_6) we detect no signals attributable to **8a.** It can be ascertained from ^{1}H NMR that K_{eq1} (**Figure 7**) is very small (estimated from the limits of integration, K_{eq1} < 0.05) and the equilibrium of tautomers lies well towards the keto form **1**. As noted above, in highly-basic aqueous solutions of **1**, the charge-minimal enolate **8b** begins to appear in substantially concentrations placing a lower-boundary of pK_a ~15 for **1**. In the absence of base, the mechanism of H-D exchange **1** to **1**-d_2 in CD_3OD most likely engages substantial equilibrium concentrations **8a** to allow rapid exchange of the CH_2 to CD_2 in deuteric solvents within less than 2 minutes at 23 °C. Estimation of an accurate pK_A of **1** is not accessible from measurements in aqueous solvents and securing the same will likely require measurements in a suitable aprotic solvent (e.g. titration in DMSO [**Error! Bookmark not defined.**,26][2]).

3. Materials and Methods

3.1. General Experimental Procedures

Inverse detected 2D NMR spectra were measured on a Jeol ECA (500 MHz) spectrometer, equipped with a 5 mm ^{1}H{^{13}C} 5 mm probe, or a Bruker Avance III (600 MHz) NMR spectrometer with a 1.7 mm ^{1}H{^{13}C} microcryoprobe. ^{13}C NMR spectra were collected on a Varian NMR spectrometer (125 MHz) equipped with a 5 mm Xsens ^{13}C{^{1}H} cryoprobe. NMR spectra were referenced to residual solvent signals, $(CD_3)_2CO$ (d_H 2.05, d_C 29.8). High-resolution ESITOF analyses were carried out on an Agilent 1200 HPLC coupled to an Agilent 6350 TOFMS. Low-resolution MS measurements were made on a Thermoelectron Surveyor UHPLC coupled to an MSD single-quadrupole detector. HPLC was performed on an Agilent 1200 HPLC. UV-vis spectra were measured on a Jasco V-630, spectrometer in quartz cells (1.00 cm pathlength, Helma). FTIR spectra were collected on thin film samples using a Jasco FTIR-4100 fitted with an ATR accessory (ZnSe plate). Optical densities (OD, *l* nm) in microplate wells were measured using a Molecular Devices Spectramax 384 Plus. Measurements of pH were made with a digital pH meter (Denver Instrument, Model 220), calibrated against standard solutions (NaH_2PO_4-Na_2HPO_4).

3.2. UV-vis Measurements

2. Bordwell values of pK_a are conventionally obtained by titration of a solution of the weak Brønsted acid in DMSO with its non-nucleophilic conjugate base, 'dimsyl sodium' ($CH_3(S{=}O)CH_2^-$ Na^+) with Ph_3CH as indicator [**Error! Bookmark not defined.**] where a colored end point is presented by the deep-red Ph_3C^- anion. In the case of **1**, the high color of the substrate and its conjugate base should lend itself to 'self-indicating'.

 doi:10.20944/preprints202307.0956.v1

Standard solutions of accurately-weighed **1** and **6b** were prepared in volumetric flasks and used for serial dilutions to the final working concentrations in specified media, either pure HPLC grade solvent (DCM, DMSO, acetone, DMF – see Supporting Information for **6b** in acetone) or mixtures of aqueous HPLC solvents of defined H_2O composition.

3.3. Synthesis of Merocyanine Dye (6b) ***[Error! Bookmark not defined.]***

Iodomethane (3.11 mL, 50 mmol) was slowly added to a cold mixture of 4-methylpyridine (4.86 mL, 50 mmol) and 2-propanol (5 mL). The stirred mixture was heated at reflux overnight. Removal of the solvent gave the crude 4-methylpyridinium methiodide (10.23 g) as an off-while solid. A portion of the latter salt (3.00 g, 12.8 mmol), 4-hydroxybenzaldehyde and piperidine (1.06 mL, 10.7 mmol) were dissolved in anhydrous EtOH (16 mL) and heated at reflux overnight, with stirring. Upon cooling, a red precipitate was deposited. The red solid was filtered (Büchner funnel) and dissolved in KOH solution (0.2 M, 17 mL, 15 mmol) and heated with stirring for 30 min. Blue-red shiny crystals were recovered by filtration, washed with a little cold water, and dried to give of **6b** (2.00 g, 65%). The ^{1}H NMR of the sample was consistent with the expected product.

3.4. H-D Exchange Measurements of 1 by ESIMS

A sample of petrosamine (**1**) was rapidly dissolved in CD_3OD (23 °C). An aliquot of the solution was immediately introduced into the inlet of the TOF mass spectrometer and the ratios of **1**-d_0, **1**-d_1 and **1**-d_2 were measured 'on the fly' from the corresponding molecular ion intensities $[M]^+$ normalized to the $[M]^+$ of a solution of **1** in CH_3OH at the same concentration. Subsequent measurements were made at 15 s intervals over a total reaction time of 90 s. See **Figure 7** and S6.

4. Conclusions

Evidence supports that the major tautomer of petrosamine is the keto form **1**, both in solution and solid states. While the enol form **8a** was not detectable by ^{1}H NMR in DMSO-d_6, it is nevertheless likely to be responsible for H-D exchange of **1** in deuteric solvents. The exceptional solvatochromism of **1** is best attributable to charge delocalized resonance forms **1a** and **1d** – partial structures seen within **1** that are analogous to Brooker merocyanine dyes [**Error! Bookmark not defined.**]. As with the latter, the hyposochromic solvents effects mostly correlate with polar-solvent stabilization of the ground state (HOMO) and attribution to the color changes of **1**. The complete isotopic exchange of the C6 CH_2 group in **1** to CD_2 in deuterated solvent under ambient conditions is supported by ^{1}H NMR and fast-sampled ESIMS measurements. The exchange mechanism likely proceeds through rapid acid-catalyzed keto-enol tautomerism.

Refinement of the molecular structure of **1** by QM methods maps the electron delocalization and accompanying charge distribution in **1**. These and other refinements complement computational docking studies that can lend more precise definition of host-guest interactions of **1** in its cognate enzyme active site. In turn, these observations may assist in the design and synthesis of new AChE inhibitors based on the pyridoacridine skeleton: a privileged alkaloid molecular framework produced exclusively by marine invertebrates.

Supplementary Materials: The following supporting information can be downloaded at the website of this paper posted on Preprints.org. FTIR of merocyanine **6b**, pH dependent UV-vis spectra of **1** FTIR of merocyanine **6b** and raw data (ESIMS) for H-D exchange rate studies of **1**.

Author Contributions: C.G. carried out the experimental work with consultation from T.F.M. The manuscript was co-written by C.G. and T.F.M.

Funding: The 500 MHz NMR spectrometer and the HPLC TOFMS were purchased with funding from the NSF (Chemical Research Instrument Fund, CHE0741968) and the NIH Shared Instrument Grant (S10RR025636) programs, respectively. This work was supported by a grant from NIH (AI1007786). This research was supported by the Academic Senate of UC San Diego.

Institutional Review Board Statement: Not applicable.

 doi:10.20944/preprints202307.0956.v1

Data Availability Statement: Original data will be made available upon reasonable request.

Acknowledgments: We are most grateful for a generous gift of petrosamine (**1**) from P. Stout (Sirenas Marine Discovery, LLC, San Diego, CA). We thank C. Perrin (UCSD) for insightful discussions and N. Goodyear for technical assistance.

Conflicts of Interest: The authors declare no conflict of interest.

References

1. Molinski, T. F.; Faulkner, D. J. Petrosamine, a Novel Pigment from the Marine Sponge *Petrosia* sp. *J. Org. Chem.* **1988**, *53*, 1341-1343.
2. Molinski, T. F. Marine Pyridoacridine Alkaloids: Structure, Synthesis, and Biological Chemistry. *Chem. Rev.* **1993**, *93*, 1825-1838.
3. Schmitz, F. J.; Agarwal, S. K.; Gunasekera, S. P.; Schmidt, P. G.; Shoolery, J. N. Amphimedine, New Aromatic Alkaloid from a Pacific Sponge, *Amphimedon* sp. Carbon Connectivity Determination from Natural Abundance ^{13}C-^{13}C Coupling Constants. *J. Am. Chem. Soc.* **1983**, *105*, 4835-4836.
4. Marshall, K. M.; Barrows, L. R. Biological activities of pyridoacridines. *Nat. Prod. Rep.* **2004**, *21*, 731-751.
5. Nukoolkarn, V. S.; Saen-oon, S.; Rungrotmongkol, T.; Hannongbua, S.; Ingkaninan, K.; Suwanborirux, K. Petrosamine, a potent anticholinesterase pyridoacridine alkaloid from a Thai marine sponge *Petrosia* n. sp. *Bioorg. Med. Chem.* **2008**, *16*, 6560-6567.
6. Carroll, A. R.; Ngo, A.; Quinn, R. J.; Redburn, J.; Hooper, J. N. A. Petrosamine B, an Inhibitor of the *Helicobacterpylori* Enzyme Aspartyl Semialdehyde Dehydrogenase from the Australian Sponge *Oceanapia* sp. *J. Nat. Prod.* **2005**, *68*, 804-806.
7. Wei, X.; Bugni, T. S.; Harper, M. K.; Sandoval, I. T.; Manos, E. J.; Swift, J.; Van Wagoner, R. M.; Jones, D. A.; Ireland, C. M. Evaluation of Pyridoacridine Alkaloids in a Zebrafish Phenotypic Assay. *Mar. Drugs* **2010**, *8*, 1769-1778.
8. Choi, D-Y.; Choi, H. Natural products from marine organisms with neuroprotective activity in the experimental models of Alzheimer's disease, Parkinson's disease and ischemic brain stroke: their molecular targets and action mechanisms. *Arch. Pharm. Res.* **2015**, *38*, 139-170.
9. See Supporting information of Ref. [**Error! Bookmark not defined.**]
10. Exchange of ^{1}H-^{13}C for ^{2}H-^{13}C results in dramatic attenuation of the ^{13}C signal due to quadrupolar relaxation, and absence of the heteronuclear nOe, among other effects.
11. Brooker, L. G. S.; Heyes, G. H.; Sprague, R. H.; Van Dyke, R. H.; Van Lare, E.; Van Zandt, G.; White, F. L. Studies in the Cyanine Dye Series. XI. The Merocyanines. *J. Am. Chem. Soc.* **1951**, *73*, 5326-5332.
12. Brooker, L. G. S.; Heyes, G. H.; Sprague, R. H.; Van Dyke, R. H.; Van Lare, E.; Van Zandt, G.; White, F. L.; Cressman, H. W. J.; Dent, S. G. Color and Constitution. X. Absorption of the Merocyanines *J. Am. Chem. Soc.* **1951**, *73*, 5332-5350.
13. Other possible resonance forms, for example invoking electron donation from Br, are considered only minor contributors.
14. Simpson, W.T. A Mathematical Treatment of the Color of the Merocyanine Dyes. *J. Am. Chem. Soc.* **1951**, 73, 5359-5356.
15. Morley, J. O.; Morley, R. M.; Docherty, R.; Charlton, M. H. Fundamental Studies on Brooker's Merocyanine. *J. Am. Chem. Soc* **1997**, *119*, 10192-10202.
16. Minch, M.J.; Sadiq Shah, S. A Merocyanin Dye Preparation for the Introductory Organic Laboratory. *J. Chem. Educ.* **1977**, *54*, 709.
17. We confirm the solvatochromism of one example, ***i***, by synthesis and its solvent-dependent UV-vis properties. See Supporting Information.
18. Hasselbalch, K.A. Die Berechnung der Wasserstoffzahl des Blutes aus der freien und gebundenen Kohlensäure desselben, und die Sauerstoffbindung des Blutes als Funktion der Wasserstoffzahl. *Biochem. Z.* **1917**, *78*, 112-114.
19. Bordwell, F.K.; Harrelson Jr., J.A. Acidities and homolytic bond dissociation energies of the αC—H bonds in ketones in DMSO. *Can. J. Chem.* **1990**, *68*, 1714-1718.
20. Bordwell, F.G. Equilibrium acidities in dimethyl sulfoxide solution. *Acc. Chem. Res.* **1988**, *21*, 456-463.
21. https://organicchemistrydata.org/hansreich/resources/pka/pka_data/pka-compilation-reich-bordwell.pdf
22. Chiang, Y.; Kresge, J.; Wirz, J. Flash-Photolytic Generation of Acetophenone Enol. The Keto-Enol Equilibrium Constant and pKa of Acetophenone in Aqueous Solution. *J. Am. Chem. Soc.* **1984**, *106*, 6392-6395.
23. Valpuesta, M.; Díaz, A.; Suau, R. Coulteroberbinone, a quaternary isoquinoline alkaloid from *Romneya coulteri*. *Phytochemistry* **1999**, *51*, 1157-1160.
24. Guthrie, J. P.; Cossar, J.; Klym, A. p*K*a values for substituted acetophenones: values determined by rates of halogenation. *Can. J. Chem*. **1987**, *65*, 2154-2159.

 doi:10.20944/preprints202307.0956.v1

25. Novak, M.; Marc Loudon, G. Aminolysis of Acetoxystyrenes. The pK_a of Acetophenones in Aqueous Solution. *J. Am. Chem. Soc.* **1976**, *98*, 3591-3597.
26. Steiner, E.C.; Gilbert, J.M. The Acidities of Weak Acids in Dimethyl Sulfoxide. *J. Am. Chem. Soc.* **1963**, *85*, 3054-3055.